Dynamical Signatures of Edge-State Magnetism on Graphene Nanoribbons

Hélène Feldner, Zi Yang Meng, Thomas C. Lang, Fakher F. Assaad, Stefan Wessel, and Andreas Honecker

Dynamical Signatures of Edge-State Magnetism on Graphene Nanoribbons

Hélène Feldner,[1, 2] Zi Yang Meng,[3] Thomas C. Lang,[4] Fakher F. Assaad,[4] Stefan Wessel,[3] and Andreas Honecker[2]

[1]*Institut de Physique et Chimie des Matériaux de Strasbourg, UMR7504,*
CNRS-UdS, 23 rue du Loess, BP43, 67034 Strasbourg Cedex 2, France
[2]*Institut für Theoretische Physik, Georg-August-Universität Göttingen,*
Friedrich-Hund-Platz 1, 37077 Göttingen, Germany
[3]*Institut für Theoretische Physik, Universität Stuttgart, 70550 Stuttgart, Germany*
[4]*Institut für Theoretische Physik und Astrophysik,*
Universität Würzburg, Am Hubland, 97074 Würzburg, Germany
(Dated: January 10, 2011; revised March 27, 2011)

We investigate the edge-state magnetism of graphene nanoribbons using a combination of projective quantum Monte Carlo simulations and a self-consistent mean-field approximation of the Hubbard model. Static magnetic correlations are found to be short-ranged. Nevertheless, the correlation length increases so rapidly with the width of the ribbon that already for ribbons of moderate widths we observe a strong trend towards mean-field type ferromagnetic correlations at a zigzag edge. These ferromagnetic correlations are furthermore shown to be accompanied by a dominant low-energy peak in the local spectral function and we propose that this can be used to detect edge-state magnetism by scanning tunneling microscopy experiments. Finally, we present results for the dynamic spin structure factor at the edge of a ribbon and verify the presence of an approximately linearly dispersing collective magnon-like mode at low energies that decays into Stoner modes beyond the energy scale where it merges into the particle-hole continuum at higher energies.

Graphene is regarded as a promising candidate for future electronics. The electronic properties of nanodevices based on this material are in a large part governed by their edge structure. Besides their potential for nanoelectronics and spintronics [1–5], graphene nanoribbons exhibit a remarkable interplay of low dimensionality, a bipartite lattice and electron-electron interactions. One of the most fundamental predictions for graphene nanoribbons (with zigzag edges) is the possibility of spontaneous edge-state magnetism, whereas bulk graphene is nonmagnetic [6–12]. Although electron-electron interactions are crucial for the emergence of edge-state magnetism, essentially all these predictions are based on mean-field type approximations. While such mean-field approximations were found – by comparing to numerical exact results – reliable at least for certain quantities and in the weak-coupling regime [13] on small honeycomb clusters, Lieb's theorem predicts no net magnetization for a bipartite system at half filling [14] and the Mermin-Wagner theorem [15] actually forbids true long-range order for a ribbon with a fixed finite width. This is consistent with a sigma-model treatment which predicts a spin gap, i.e., a finite spin-spin correlation length for an even number of zigzag lines [16]. Furthermore, a numerical study indeed found a quite short correlation length in the case of two zigzag lines [17].

In view of this puzzling situation, and given the growing experimental effort toward probing the magnetism of graphene nanoribbons, we believe that there is need for an accurate numerical treatment of the Hubbard model description. Here we present projective ground-state quantum Monte Carlo simulations [18] and compare them with a self-consistent mean-field theory (MFT) [13].

For narrow ribbons we find indeed a finite correlation length, i.e., the static magnetism is an artifact of the mean-field approximation. However, with increasing width we observe a fast convergence of the qualitative behavior of the correlation functions towards the MFT result corresponding to strong ferromagnetic ordering tendencies. Since the ferromagnetic order is not static but subject to fluctuations, we next explore the dynamical properties of the nanoribbons, focusing both on local and momentum-resolved single-particle and spin spectral functions. We find that the single-particle spectral function on the edge exhibits a low-energy peak as a dynamic signature of the edge-state magnetism. The spin spectral functions reveal the onset of magnon-like excitations on top of the fluctuating magnetic background along the zigzag edge. We exhibit a linear contribution to their low-energy dispersion [7, 19, 20] and, even more interestingly, the damping of this mode into the Stoner continuum [20].

The ribbon geometry considered here is depicted in the inset of Fig. 1. We employ periodic boundary conditions at the armchair edge and open boundary conditions at the zigzag edge. L and W denote the length and the width of the ribbon, respectively. L is measured in units of lattice vector $\mathbf{a}_1 = (\sqrt{3}, 0)$ and W is the number of zigzag legs of the ribbon. The carbon-carbon bond length is set to unity.

The Hamiltonian of the Hubbard model reads

$$H = -t \sum_{\langle i,j \rangle, \sigma} (c_{i,\sigma}^{\dagger} c_{j,\sigma} + c_{j,\sigma}^{\dagger} c_{i,\sigma}) + U \sum_{i} n_{i,\uparrow} n_{i,\downarrow} \quad (1)$$
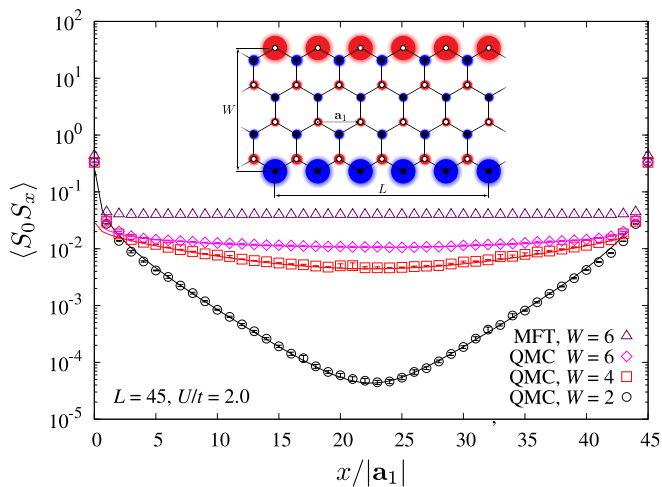
FIG. 1. (Color online) Real-space spin-spin correlation function along the zigzag edge of ribbons. Points are the QMC and MFT data and lines are the fits with Eq. (2). Inset: Geometry of the graphene nanoribbon with zigzag edge, $L = 6$, $W = 4$, and lattice size $N = 2 \times L \times W = 48$. Red and blue circles represent the positive and negative values of the local magnetization $\langle S_i^z \rangle = \frac{1}{2} \langle n_{i,\uparrow} - n_{i,\downarrow} \rangle$, calculated from MFT at $U/t = 2$. Radii are proportional to the magnitude.
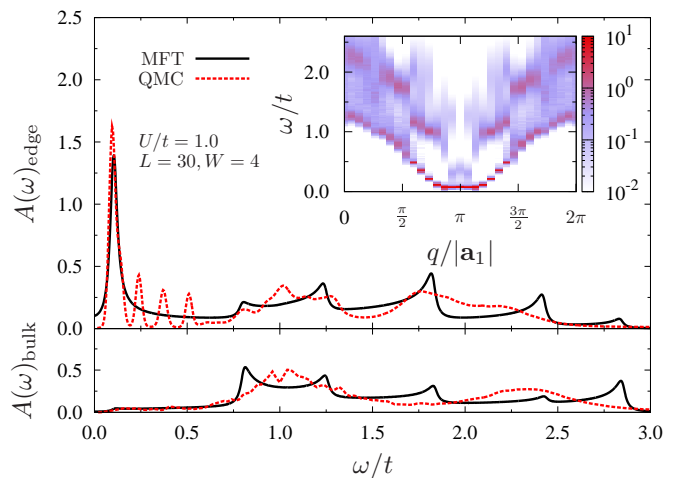

FIG. 2. (Color online) Spectral functions of a width $W = 4$ ribbon at $U/t = 1$. QMC data is for a ribbon of length $L = 30$ whereas MFT corresponds to the thermodynamic limit. The inset shows QMC results for the momentum-resolved spectral function $A(q, \omega)$ along the zigzag edge, while the main panel shows the local spectral function $A(\omega)$ subject to a Lorentzian broadening $\Delta \omega = 0.02\, t$. Note the prominent low-energy peak in $A(\omega)_{\text{edge}}$ at $\omega/t \approx 0.1$ which is absent in $A(\omega)_{\text{bulk}}$.

with $\langle i, j \rangle$ nearest neighbors on the lattice, $\sigma = \uparrow, \downarrow$ and $n_i = c_i^\dagger c_i$. We concentrate on half filling, i.e., the number of electrons is equal to the number of lattice sites. MFT for the 2D periodic honeycomb lattice yields a transition from a semimetal to an antiferromagnet at $U_c/t = 2.23$ [21] whereas QMC reveals a metal-insulator transition for $U_{c1}/t = 3.5(1)$ and a further nonmagnetic insulator-antiferromagnetic insulator for $U_{c2}/t = 4.3(1)$ [22]. In this work, we focus on the interaction range $U/t \leq 2$ since we are interested in the behavior of the system in the weak-coupling regime. Estimates of the local Coulomb repulsion U for graphene [12] lie around $U/t = 1$ and thus fall indeed into this regime.

The inset of Fig. 1 shows the MFT result for the local magnetization at the edge of a $W = 4$, $L = 6$ ribbon at $U/t = 2$ and illustrates the edge-state magnetism which is expected for weak Coulomb interactions $U/t > 0$ [6–12]. This is reflected by the MFT result for the spin-spin correlation function which is shown by triangles for $W = 6$, $L = 45$, and $U/t = 2$ in the main panel of Fig. 1: the correlation function rapidly approaches a constant value as a function of distance x along the edge with very little dependence on the width W of the ribbon (not shown).

By contrast, the QMC results for the static spin-spin correlation function shown in the main panel of Fig. 1 exhibit a clear decay, at least for narrow ribbons with $W = 2$ (circles) and 4 (squares). Note that the rapid decay for $W = 2$ is consistent with a previous DMRG study [17]. However, as the width increases, the decay becomes slower and the QMC result for $W = 6$ in Fig. 1

(diamonds) is already qualitatively similar to the MFT result.

For a more quantitative analysis we fit the QMC data for the longest available ribbons with a function combining exponential and power-law behavior

$$\langle S_0 S_x \rangle = C \left(x^{-\eta} e^{-x/\xi} + (L|\mathbf{a}_1| - x)^{-\eta}\, e^{-(L|\mathbf{a}_1| - x)/\xi} \right). \tag{2}$$

From a fit for $L = 60$ at $W = 2$ we estimate $\xi/|\mathbf{a}_1| = 4.0 \pm 1$ and $\eta = 0.5 \pm 0.3$ and at $W = 4$ the $L = 54$ data yields $\xi/|\mathbf{a}_1| = 15 \pm 4$ and $\eta = 0.2 \pm 0.15$. At $W = 6$ it is no longer possible to distinguish the correlation length from infinity or the exponent η from zero for the largest available system size within our study ($L = 45$). Indeed, the $W = 6$ QMC data can equally well be fitted by predictions based on an infinite correlation length. We thus arrive at a picture similar to even-leg spin ladders [23] or integer spin-S quantum chains [24]: ribbons with even W have a finite spin-spin correlation length [16], but the correlation length rapidly grows with W such that for practical purposes it can be considered infinite for $W \gtrsim 6$. In this sense edge-state magnetism is found already for ribbons of moderate widths. In order to check if MFT becomes also quantitatively accurate for wider ribbons, one would need to go beyond the system sizes which we can presently access by QMC.

Since the ferromagnetic behavior at the edges remains fluctuating in a proper treatment of the Hubbard model (1), we now turn to the dynamic properties. In this respect, the local single-particle spectral function $A(\omega)$ is a particularly important observable since it can be ob-
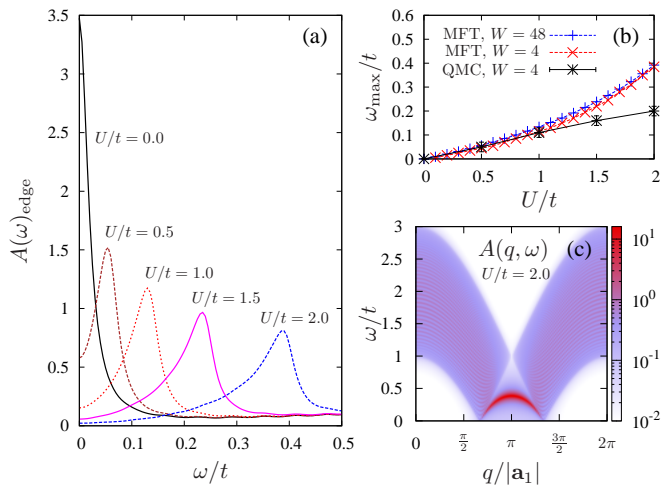
FIG. 3. (Color online) (a) Single-particle spectral function $A(\omega)_{\text{edge}}$ for several values of U/t and a ribbon of width $W = 48$. (b) Comparison of the position ω_{max} of the maximum of $A(\omega)_{\text{edge}}$ between MFT for $W = 4, 48$ and QMC for $W = 4$ and $L = 30$. (c) $A(q, \omega)_{\text{edge}}$ for a ribbon with $W = 48$ at $U/t = 2$. Unless stated otherwise, results are based on MFT for long ribbons and a Lorentzian broadening $\Delta\omega = 0.02\,t$.

served in scanning tunneling microscopy (STM) experiments [25, 26]. However, to the best of our knowledge, previous theoretical studies of the interplay of edge-state magnetism and spectral functions of graphene ribbons are restricted to density-functional approaches [11, 27] with an inherent mean-field type approximation. In QMC we measure the momentum-resolved Green's function in imaginary time $G(q, \tau)$, and then apply a stochastic analytical continuation scheme [28, 29] to rotate $G(q, \tau)$ on the τ-axis to $A(q, \omega)$ on the ω-axis. Finally, the local spectral function $A(\omega)$ is obtained by integration over the momentum q along the ribbon direction.

Fig. 2 shows the single-particle spectral function both on the zigzag edge $A(\omega)_{\text{edge}}$ and inside the bulk $A(\omega)_{\text{bulk}}$ for ribbon of width $W = 4$ at $U/t = 1$. The local spectral functions in the main panel were subjected to a Lorentzian broadening of $\Delta\omega = 0.02\,t$. $A(\omega)_{\text{edge}}$ exhibits a dominant low-energy peak at $\omega/t \approx 0.1$ which is absent in $A(\omega)_{\text{bulk}}$. This peak can be traced to a flat region of a single-particle dispersion visible in $A(q, \omega)_{\text{edge}}$ (compare the inset in Fig. 2). The agreement between MFT and QMC is excellent for this low-energy peak and the overall agreement is also good at higher energies. The three additional sharp features in the QMC result for $A(\omega)_{\text{edge}}$ in the region $0.2 < \omega/t < 0.6$ can be traced to a finite-size momentum discretization effect and are reproduced by MFT if the latter is also restricted to a length $L = 30$ ribbon. We conclude that the agreement between MFT and QMC for $A(\omega)$ is remarkable even at a quantitative level, at least for weak interactions $U/t \lesssim 1$.

Having gained confidence in the accuracy of the MFT results for $A(\omega)$, we use it to analyze a bigger and

more realistic system with $W = 48$, corresponding to a graphene nanoribbon of 10 nm width. The evolution of the low-energy peak on the edge with the Coulomb repulsion is shown in Fig. 3(a). The energy ω_{max} corresponding to the maximum intensity of the spectral function increases with the Coulomb repulsion U and is located at $\omega_{\text{max}} = 0$ only for $U = 0$, i.e., the non-interacting system. In combination with the fact that this peak exists only on the ferromagnetic edge (compare Fig. 2) we conclude that it is a clear dynamic signature of edge-state magnetism. Fig. 3(b) demonstrates that ω_{max} is insensitive to the actual width of the ribbon and confirms that MFT is accurate for $U/t \lesssim 1$ (the fact that MFT becomes less accurate as one approaches the mean-field phase transition at $U_c/t = 2.23$ [21] is not surprising).

The momentum-resolved spectral function (shown in Fig. 3(c) for $U/t = 2$) reveals that the feature at ω_{max} can be traced to the maximum of a single-particle band at $q/|\mathbf{a}_1| = \pi$ where large matrix elements and a Van Hove singularity combine to yield a maximum intensity of the local spectral function. The true single-particle gap Δ_{sp} is located in the vicinity of $q/|\mathbf{a}_1| = 2\pi/3$ and $4\pi/3$. For the $W = 48$ ribbon shown in Fig. 3 it is only $\Delta_{sp}/t = 0.037$ for $U/t = 2$, resulting in a fill-in of spectral weight in the local density of states below the 'pseudo-gap' ω_{max} (compare Fig. 3(a)). The value of the single-particle gap Δ_{sp} depends strongly on the width of the ribbon; for the $W = 4$ ribbon shown in Fig. 2 it is quite close to the pseudo-gap ω_{max}. Note that the data in Fig. 3(a) is subjected to a broadening $\Delta\omega = 0.02\,t$. With a higher energy resolution, one would observe further features, in particular another Van Hove singularity at Δ_{sp}, albeit with a much smaller weight than at ω_{max}.

Another probe to exhibit the peculiar magnetic properties of zigzag nanoribbons is provided by the spin spectral function $S(q, \omega)$ on the edge. From the enhanced ferromagnetic correlations along the zigzag edge at finite values of U, one might expect $S(q, \omega)$ to exhibit collective spin-wave (magnon) excitations characteristic of a ferromagnetic background, with a quadratic low-energy dispersion relation near $q = 0$. However, as pointed out in Refs. [7, 20], the magnetic excitations are affected by the antiferromagnetic coupling between the two edges of the nanoribbon that is mediated by the bulk conduction electrons. These antiferromagnetic correlations result in a linear contribution to the dispersion at small wave vectors (see also Ref. [19]). Furthermore, for energies entering the particle-hole continuum, the collective modes can decay into strongly damped Stoner modes [20].

Our QMC data in Fig. 4 indeed exhibit such a scenario for a ribbon with $W = 4$: an approximately linearly dispersing sharp mode is observed up to a wave vector $q/|\mathbf{a}_1| \approx 0.5\,\pi$ with a threshold energy $\omega_{th}/t = 0.42 \pm 0.04$, compatible with twice the corresponding single-particle gap of $\Delta_{sp}/t = 0.2 \pm 0.02$. The inset of
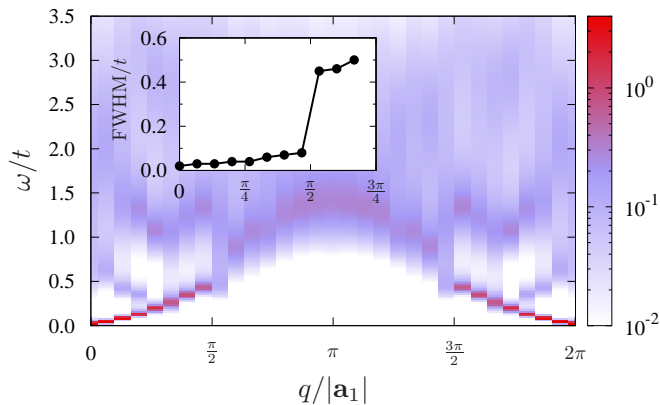
FIG. 4. (Color online) QMC results for the spin spectral function $S(q,\omega)$ along the edge of a zigzag ribbon with $L = 30, W = 4$ and $U/t = 2$. The inset shows the linewidth (FWHM) of the dominant mode in $S(q,\omega)$ as a function of momentum q.

Fig. 4 shows the corresponding evolution of the linewidth (FWHM) of this low-energy mode that drastically increases beyond $q/|\mathbf{a}_1| \approx 0.5\,\pi$.

In summary, we have investigated the static as well as dynamic properties of graphene nanoribbons with zigzag edges. Upon closer inspection, true ferromagnetic long-range order at the zigzag edge [6–12] of a finite-width ribbon turns out to be absent [14–17], yet there are strong ferromagnetic correlations which are essentially long range but for the narrowest ribbons. As a next step, we have identified a dominant low-energy peak in the local spectral function as a dynamic signature of edge-state magnetism, thus providing a theoretical guide for further STM and spin-resolved STM experiments. The agreement between QMC and MFT for the local spectral function is remarkably accurate for moderate Coulomb interactions, justifying a description of realistic geometries within a MFT framework. In particular, we have demonstrated that the position of the dominant low-energy peak at the zigzag edge of a nanoribbon is controlled mainly by the Coulomb interaction U such that STM experiments can be used to deduce the appropriate value for graphene. Lastly, we have presented QMC results for the dynamic spin structure factor at the edge of a width $W = 4$ ribbon and demonstrated the presence of an approximately linearly dispersing low-energy collective spin-wave excitations [7] that decay upon entering the particle-hole continuum [20].

Note added: After completion of this work, we became aware of Ref. [30] which has observed low-energy spectral features by STM and compared those to MFT for isolated chiral graphene nanoribbons.

---

[1] Y.-W. Son, M. L. Cohen, and S. G. Louie, Phys. Rev. Lett. **97**, 216803 (2006).
[2] Y.-W. Son, M. L. Cohen, and S. G. Louie, Nature **444**, 347 (2006).
[3] B. Trauzettel, D. V. Bulaev, D. Loss, and G. Burkard, Nature Physics **3**, 192 (2007).
[4] O. V. Yazyev and M. I. Katsnelson, Phy. Rev. Lett. **100**, 047209 (2008).
[5] F. Muñoz-Rojas, J. Fernández-Rossier, and J. J. Palacios, Phys. Rev. Lett. **102**, 136810 (2009).
[6] M. Fujita, K. Wakabayashi, K. Nakada, and K. Kusakabe, J. Phys. Soc. Jpn. **65**, 1920 (1996).
[7] K. Wakabayashi, M. Sigrist, and M. Fujita, J. Phys. Soc. Jpn. **67**, 2089 (1998).
[8] K. Wakabayashi, M. Fujita, H. Ajiki, and M. Sigrist, Phys. Rev. B **59**, 8271 (1999).
[9] J. Fernández-Rossier and J. J. Palacios, Phys. Rev. Lett. **99**, 177204 (2007).
[10] S. Bhowmick and V. B. Shenoy, J. Chem. Phys. **128**, 244717 (2008).
[11] J. Jiang, W. Lu, and J. Bernholc, Phys. Rev. Lett. **101**, 246803 (2008).
[12] O. V. Yazyev, Rep. Prog. Phys. **73**, 056501 (2010).
[13] H. Feldner, Z. Y. Meng, A. Honecker, D. Cabra, S. Wessel, and F. F. Assaad, Phys. Rev. B **81**, 115416 (2010).
[14] E. H. Lieb, Phys. Rev. Lett. **62**, 1201 (1989).
[15] N. D. Mermin and H. Wagner, Phys. Rev. Lett. **17**, 1133 (1966).
[16] H. Yoshioka, J. Phys. Soc. Jpn. **72**, 2145 (2003).
[17] T. Hikihara, X. Hu, H. H. Lin, and C. Y. Mou, Phys. Rev. B **68**, 035432 (2003).
[18] F. F. Assaad and H. G. Evertz, Lect. Notes Phys. **739**, 277 (2008).
[19] J.-S. You, W.-M. Huang, and H.-H. Lin, Phys. Rev. B **78**, 161404 (2008).
[20] F. Culchac, A. Latgé, and A. T. Costa, (2010), arXiv:1007.3285v2.
[21] S. Sorella and E. Tosatti, Europhys. Lett. **19**, 699 (1992).
[22] Z. Y. Meng, T. C. Lang, S. Wessel, F. F. Assaad, and A. Muramatsu, Nature **464**, 847 (2010).
[23] E. Dagotto and T. M. Rice, Science **271**, 618 (1996).
[24] S. Todo and K. Kato, Phys. Rev. Lett. **87**, 047203 (2001).
[25] Y. Niimi, T. Matsui, H. Kambara, K. Tagami, M. Tsukada, and H. Fukuyama, Phys. Rev. B **73**, 085421 (2006).
[26] M. M. Ugeda, I. Brihuega, F. Guinea, and J. M. Gómez-Rodríguez, Phys. Rev. Lett. **104**, 096804 (2010).
[27] H. Y. He, Y. Zhang, and B. C. Pan, J. Appl. Phys. **107**, 114322 (2010).
[28] A. W. Sandvik, Phys. Rev. B **57**, 10287 (1998).
[29] K. S. D. Beach, (2004), arXiv:cond-mat/0403055v1.
[30] C. Tao, L. Jiao, O. V. Yazyev, Y.-C. Chen, J. Feng, X. Zhang, R. B. Capaz, J. M. Tour, A. Zettl, S. G. Louie, H. Dai, and M. F. Crommie, (2011), arXiv:1101.1141v1.